This article has been accepted for publication in a future issue of this journal, but has not been fully edited. Content may change prior to final publication. Citation information: DOI 10.1109/TII.2017.2682101, IEEE Transactions on Industrial Informatics



# Optimal Protection Coordination for Microgrids Considering N−1 Contingency

Khaled A. Saleh, *Student Member, IEEE,* H. H. Zeineldin, *Senior Member, IEEE,* and Ehab F. El-Saadany *Senior Member, IEEE*.

***Abstract*—Usually, protection coordination problems are solved under the assumption that the network topology is fixed. Yet, in practice, any power system can encounter changes in the network topology due to transient events. These transient events can be in the form of line or generation source outage. Furthermore, in the presence of distributed generation, the network topology can change depending on whether the system is operating in the grid-connected or islanded mode. Thus, it is essential to consider all possible network topologies while designing a protection scheme for distribution systems with DG. In this paper, the protection coordination problem is solved to determine the optimal relay settings considering N−1 contingency which can result from a single line, distributed generation unit, or substation outage. In addition, the relays are designed taking into account both grid-connected and islanded operation modes. The problem has been formulated as a mixed integer nonlinear programming problem including coordination constraints corresponding to the various possible outages. The proposed approach is tested on a 9-bus radial distribution system and on the IEEE 14-bus meshed distribution system, both equipped with distributed generation units.**

***Index Terms*—Distributed generation, optimization method, micro-grid, N−1 contingency, protection coordination.**

## I. Introduction

PROTECTION schemes aim to protect power systems against faults by quickly isolating as little of the system as possible. The typical design of any protection scheme involves associating primary protective devices that are backed up by other protective devices for each line on the system. For a fault occurring on a line, the primary protective devices should operate. However, in case they fail to operate, the backup protective devices should operate after a specific time interval. The process of determining the sequence of operation of each primary/backup protective device pair associated with each fault location is known as protection coordination.

Conventional distribution power systems have a radial structure in which the power flows from the substation to the loads in one direction [1]. Such systems rely on overcurrent relays (OCRs) as the main means of protection. Yet, the nature of distribution systems have changed with the recent drive towards smart grids and interest in integration of distributed generation (DG) units. Some modern distribution systems can either have DG units connected to the conventional radial structure or to a meshed structure that resembles interconnected sub-transmission systems [2], [3]. This has led to the concept of micro-grids where a distribution system can be supplied by a group of DG units with or without a grid connection. All the system configurations mentioned above will experience bidirectional flow of short circuit currents during fault conditions [4]. Thus, in such systems, protection schemes based on directional overcurrent relays (DOCRs) are utilized [5]–[12].

The tripping operation of a DOCR is usually governed by an inverse time current characteristic that is dependent on the time dial setting ($TDS$) and the pickup current setting ($I_p$). Microprocessor-based DOCRs offer users to select from a range of continuous TDS settings and discrete Ip tap settings. Over the past few decades, optimization techniques have been applied to solve the protection coordination problem. In [13]–[17], the protection coordination problem was formulated as a linear programming (LP) problem and was solved using the simplex, two-phase simplex, and dual simplex methods. However, such formulation was achieved by assuming known Ip settings and solving for TDS. On the other hand, the problem was formulated as a nonlinear programming (NLP) problem and was solved using Sequential Quadratic Programming (SQP) algorithm [18], genetic algorithm (GA) [8], and hybrid GA-NLP [19]. Yet, these approaches assume that $I_p$ settings are continuous variables. Alternatively, in [20] and [21], a mixed integer nonlinear programming (MINLP) problem formulation was proposed that was solved by particle swarm optimization (PSO), and hybrid GA, respectively.

Power systems may experience transient changes in the network topology due to line or generation unit outage contingencies. Such outages can be caused by maintenance activities, network reconfiguration, and fault isolation actions [21]. According to NERC reliability standards [22], outages of any line or generator (excluding the outage of any radial line) is considered as an $N-1$ contingency case. $N-1$ contingency analysis have been widely considered in power system planning studies [23]–[25]. Additionally, the network topology of a micro-grid alters with the change in its operation mode (grid-connected or islanded mode of operation) [8]. These alterations in the network configuration might cause



K. A. Saleh is with the Electrical and Computer Engineering Department, University of Waterloo, Waterloo, ON N2L3G1, Canada e-mail:(k4saleh@uwaterloo.ca).

H. H. Zeineldin is with the Department of Electrical Engineering and Computer Science, Masdar Institute of Science and Technology, Abu Dhabi 54224, U.A.E, and currently on leave from the Faculty of Engineering, Cairo University, Giza 12316, Egypt (e-mail: hzainaldin@masdar.ac.ae).

E. F. El-Saadany is with Electrical and Computer Engineering Department, University of Waterloo, Ontario, Canada, and is currently on leave with the Petroleum Institute, Abu Dhabi, United Arab Emirates (e-mail: ehab@uwaterloo.ca).

This article has been accepted for publication in a future issue of this journal, but has not been fully edited. Content may change prior to final publication. Citation information: DOI 10.1109/TII.2017.2682101, IEEE Transactions on Industrial Informatics



improper operation of the protection scheme. In [15], [17], [21], and [26] the protection coordination problem is solved for transmission or sub-transmission systems considering all possible network topologies resulting from single line outage contingencies. This is accomplished by taking into account a set of nonlinear inequality coordination constraints corresponding to each network topology. On the other hand, [8] proposed the use of fault current limiters (FCLs) in series with the utility substations to solve the protection coordination problem for microgrids while accommodating both grid-connected and islanded modes of operation. Yet, none of the studies proposed in the literature consider line, DG units, and substation outage contingencies simultaneously while solving the protection coordination problem for microgrids (both grid-connected and islanded configurations).

This paper provides a comprehensive analysis for solving the protection coordination problem by considering $N-1$ contingency including single outage (line, substation, or DG) in addition to microgrid operation modes. The proposed method utilizes DOCRs as the main protection means and is applied to radial and meshed distribution systems that are equipped with synchronous based DG units (because they have much more profound effect on the short circuit currents magnitudes than inverter based DG units [27]). The problem is formulated as a constrained MINLP problem. Unlike existing protection coordination optimization approaches, the proposed method incorporates a new set of coordination constraints that correspond to line, substation, DG outages, as well as microgrid operation modes. All the case studies in this paper are performed on the 9-bus radial section of the Canadian Urban Benchmark distribution system and the distribution portion of the IEEE 14-bus meshed system. The results highlight the proposed approach's advantage of maintaining coordination between DOCR primary/backup pairs under various fault location and network topologies over existing protection coordination methods.

## II. Proposed Formulation For The Protection Coordination Problem

The operation time of a DOCR is usually determined by an inverse characteristic of the short circuit current magnitude passing through it. Several DOCR characteristics have been reported that usually follow either the IEEE or IEC standards. In this paper, it is assumed that all DOCRs are identical and is represented by [28]:

$$t = TDS\frac{A}{\left(\dfrac{I_{sc}}{CTR \times I_p}\right)^B - 1} \tag{1}$$

where $t$ is the tripping time (in seconds). $I_{sc}$ is the short circuit current measured at the secondary winding of the DOCR current transformer. The current transformer ratio ($CTR$) along with the discrete pickup current tap setting ($I_p$) determine the threshold current above which the DOCR operate. This threshold should be set at a value that is slightly higher than the rated load current. $TDS$ is a continuous DOCR setting that is used as a tuning parameter. The constants $A$ and $B$ are fixed parameters that determine the type of tripping curve. In line protection application, standard inverse is commonly used, and thus $A$ and $B$ are set to 0.14 and 0.02, respectively [29].

The protection coordination optimization (PCO) problem is formulated as a MINLP problem as a result of the discrete and nonlinear nature of the DOCR characteristic equation. The decision variables of this optimization problem are the TDS and Ip settings of all DOCRs. The objective of this problem is to minimize the operation times of all DOCRs while satisfying all of the coordination and relay settings constraints. According to [26], a reduction of the DOCRs primary operating time should lead to a reduction in its backup operating time because both operating times are not in conflict when considered as separate objectives. Thus, as in [17] and [21], the objective of the PCO model is to minimize the overall operating time ($T$) of the primary relays corresponding to near-end fault locations on a power system. The objective function can be represented by the following equation:

$$min \quad T = \sum_{i=1}^{N} t_i \tag{2}$$

where $N$ is the total number of DOCRs and $t_i$ is the operating time of relay $i$ due to its respective near-end fault.

A set of relay settings and coordination constraints are included in the optimization model of this problem. The $TDS$ setting for each relay is limited between a lower and upper bounds ($TDS_{i-min}$ and $TDS_{i-max}$). On the other hand, the lower bound of the pickup current tap setting ($I_{pi-min}$) for each relay is chosen so that the resultant current threshold ($CTR \times I_p$) is higher than the rated load current of the respective protected line. This ensures that each DOCR will trip only if a fault occurs. The constraints imposed on the DOCR settings can be expressed as follows:

$$TDS_{i-min} \leq TDS_i \leq TDS_{i-max} \qquad \forall i = 1, 2, \ldots N \tag{3}$$

$$I_{pi-min} \leq I_{pi} \leq I_{pi-max} \qquad \forall i = 1, 2, \ldots N \tag{4}$$

Another set of constraints are necessary to guarantee that a minimum gap in time between the operation of primary and backup DOCRs, known as coordination time interval ($CTI$), is maintained under all conditions. $CTI$ is set to 200 ms to adhere to industrial [30] and IEEE 242-2001 [31] recommended practices. The 200 ms $CTI$ takes into account the breaker operating time and the current transformer and relay errors [32]. The coordination constraints can be defined as:

$$t_{cl}^{b_x} - t_{cl}^{p} \geq CTI \qquad \forall c, [l, x] \tag{5}$$

where the superscript $p$ represents primary relays, while $b_x$ represents the corresponding backup relay $x$ (each primary relay can have $x$ backup relays). The variables $t_{cl}^{p}$ and $t_{cl}^{b_x}$ represent the primary and backup relays operating time for a fault occurring at location $l$ when $c$ network topology is effective, respectively. In this paper, the developed PCO model takes into account the coordination constraints corresponding to near-end and far-end fault locations occurring on each line

This article has been accepted for publication in a future issue of this journal, but has not been fully edited. Content may change prior to final publication. Citation information: DOI 10.1109/TII.2017.2682101, IEEE Transactions on Industrial Informatics



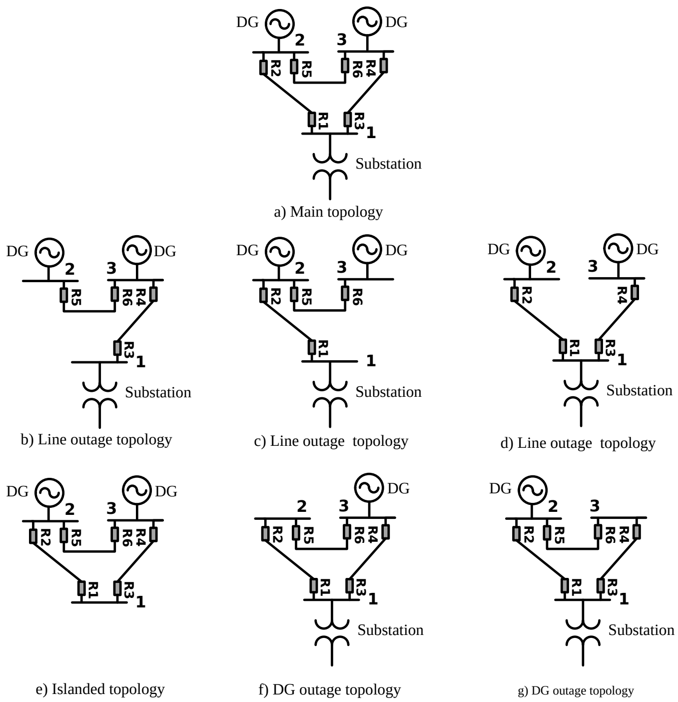

Fig. 1. Network topologies of the three bus system

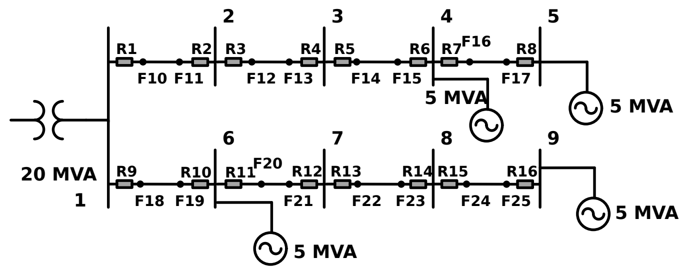

Fig. 2. Radial 9-bus Distribution System with DG units

in a power system. Furthermore, this PCO model can accommodate coordination constraints corresponding to the main network topology and all resultant topologies that are obtained from transients (single line and source outage contingencies) and operation modes (grid-connected and islanded). It is worth noting that the proposed PCO model is solved offline, where the obtained optimal settings are used as pre-defined settings for the DOCRs.

As an example, Fig. 1 shows a three bus system with a substation connected at bus 1 and two DG units connected at buses 2 and 3 respectively. It can be seen that six network topologies (Figs. 1b - 1g) are attained from the main network topology (Fig. 1a) based on single line outage contingencies (Figs. 1b–1d), single DG outage contingencies (Figs. 1f, 1g) and islanded mode of operation (Fig. 1e). Each topology results in 12 coordination constraints (due to inclusion of near-end and far-end faults) expect topologies with a single line outage (Fig. 1b, 1c, and 1d) that only have four coordination constraints. Thus, for the 3 bus system example, a total of 60 coordination constraints would be included in the PCO model.

## III. System Details and Simulation Setup

The proposed formulation for DOCR protection coordination problem is tested on a radial and looped distribution system with DG units. The next subsection presents a description of both systems under study. This is followed by a brief explanation of the developed testing models. The latter subsection presents the hybrid genetic algorithm and linear programming (GA-LP) technique used to solve the developed PCO models.

### A. Description of the Test Systems under Study

In this paper, two systems are used to test the developed PCO models. The first test system shown in Fig. 2 is based on a section (two feeders) of the Canadian Urban Benchmark 4-bus feeder distribution system [33]. All of the lines are 500 m long. This radial distribution system is fed by a utility with a short-circuit capacity of 500 MVA and X/R ratio equal to 6. The utility is connected to the system through a 20 MVA, 115kV / 12.47 kV substation transformer with 10% sub-transient reactance. Furthermore, this system is equipped with four synchronous based DG units each rated at 5MVA and has a 9.67% sub-transient reactance. Each DG unit is connected through a 480V/33 kV set-up transformer with 5% sub-transient reactance. Moreover, 16 DOCRs are used as the main protective devices in this system. In this paper, each DOCR have seven available discrete pickup current tap settings (0.5, 0.6, 0.8, 1.0, 1.5, 2.0, and 2.5) and continuous $TDS$ value that is within the range from 0.05 to 5. The $CTR$ of each DOCR in this system is 4000:5 A. This ratio is chosen to ensure that the minimum possible pickup current is higher than the rated load current. Three-phase bolted faults are performed at nodes (F10-F25) that represent the near-end and far-end fault locations on each line (Fig. 2). For each fault location two primary DOCRs are assigned where each primary has one backup DOCR. For example, if a fault occurred at node F12, the DOCRs R3 and R4 operate as primary while R1 is operating as backup for R3 and R6 is operating as backup for R4.

The second test system used in this paper is based on the distribution system part of the IEEE 14 system [34] that is shown in Fig. 3. The system is fed by the utility with a short circuit 500 MVA capacity and X/R ratio equal to 6. The utility is connected to the system through two 60 MVA 132kV/33 kV transformers connected at buses 1 and 2. Three synchronous based DG units are connected to this system. Each unit is rated at 20 MVA with 9.67% sub-transient reactance and feeds the system through a 480V/33 kV set-up transformer (5% transient reactance). This system is equipped with 16 DOCRs that have the same range of available $TDS$ and $I_p$ settings as mentioned above. Yet, in this system the $CTR$ of each DOCR is different based on the rated current passing through the respective branch. Using the same selection criteria discussed in the first test system, the $CTR$ value for each DOCR is shown in Table I. In this system, 16 nodes denoted by (F8-F23) are the locations at which bolted three phase faults are performed. Similar to the 9-bus system, each fault location is

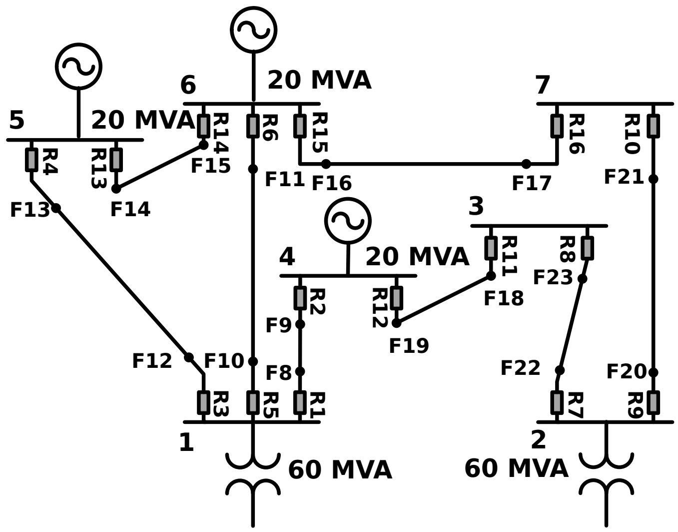


Fig. 3. IEEE 14-bus Distribution System with DG units

TABLE I
CTR OF DOCRS IN THE IEEE 14-BUS SYSTEM

| Relay | $CTR$ | Relay | $CTR$ |
|---|---|---|---|
| 1 | 1200:5 | 9 | 1200:5 |
| 2 | 1200:5 | 10 | 1200:5 |
| 3 | 1200:5 | 11 | 600:5 |
| 4 | 500:5 | 12 | 600:5 |
| 5 | 1200:5 | 13 | 200:5 |
| 6 | 1200:5 | 14 | 200:5 |
| 7 | 1000:5 | 15 | 900:5 |
| 8 | 1000:5 | 16 | 900:5 |

associated with up to two primary DOCRs. However, due to the looped nature of this system, each primary DOCR can be associated with up to two backup DOCRs.

As discussed in Section I, the different approaches proposed in the literature to solve the protection coordination problem for multiple network topologies are investigated. In addition, this paper proposes the inclusion of additional constraints to account for single line, DG outage contingencies (transients) along with the micro-grids two modes of operation. Contingencies are modelled by eliminating the parameters of the given outage from the admittance-bus matrix, which is used to compute the short-circuit currents in the system. Table II summarizes the different models studied in this paper. Model 1 is the most commonly used protection model, where the relay settings are optimally determined considering only the main system configuration [5]–[7],[9]–[12]. Model 1 was augmented in [15], [17], [21], and [26] with additional set of constraints that take into account line outages and is denoted as Model 2. Model 3, proposed in [8], considers two main configurations namely: 1) the grid-connected and 2) islanded-operation. Model 3 does not take into account line or DG outage. Model 4, however, represents the proposed model, which provides a comprehensive approach that takes into account simultaneously all of the above in addition to DG outages. It is worth nothing that the objective function for all of the above models includes the DOCRs operating times

TABLE II
DESCRIPTION OF SIMULATION MODELS

| model | Topologies Considered in the PCO Model |
|---|---|
| 1 | Main topology only |
| 2 | Main topology<br>+ all topologies due to single line outage contingencies |
| 3 | Main topology (grid-connected)<br>+ Microgrid islanded mode topology |
| 4* | Main topology<br>+ all topologies due to single line/DG outage contingencies<br>+ Microgrid islanded mode topology |

*Proposed PCO model

of the main topology only to allow for a fair performance comparison.

### B. Hybrid GA-LP Implementation

The PCO models developed in this paper are solved using a hybrid GA-LP technique that is proposed by [21]. Basically, the algorithm starts by defining the system and relay data based on the considered network topologies. Short circuit analysis is conducted on all considered network topologies and inputted to the optimization model that determines the relay settings. The optimization technique divides the formulated MINLP protection coordination problem into a nonlinear integer part (solved by GA) and a linear part (solved by LP).

Since the pickup current tap setting $I_p$ values are discrete and are the cause of nonlinearity in the problem, the GA is used to solve the PCO model considering $I_p$ values as the decision variables of this problem. Usually, in the GA, each chromosome consists of an encoded binary string. If each system has $N_1$ relays each with $N_2$ available discrete taps $I_p$, then the length of each chromosome is $L = N_1 \times N_2$. An initial population is generated consisting of a group of randomly initialized chromosomes. In this paper, the population size is assumed to be 100 individuals. The fitness of each chromosome in the population is evaluated based on the objective function and the satisfaction of the problem constraints. In order to be able to evaluate the fitness of each chromosome, the LP sub-problem, with (2) being the objective function should be solved. By decoding the information in each chromosome, the protection coordination problem is converted into a linear programming problem in which the decision variables of the problem are the TDS values for all relays. Therefore, based on the $I_p$ values obtained from each chromosome in the population, the LP sub-problem is solved to determine the corresponding $TDS$ values. Depending on the $I_p$ values passed by each chromosome, the LP sub-problem might not converge. This means that some of the coordination constraints are violated. In such cases, a fixed positive penalty value is added (since it is minimization problem) to the fitness value corresponding to these chromosomes. This will decrease the favourability of the chromosomes that result in coordination violation (LP sub-problem does not converge) over the chromosomes that result in feasible LP sub-problem. The fitness value for each chromosome can be computed using

This article has been accepted for publication in a future issue of this journal, but has not been fully edited. Content may change prior to final publication. Citation information: DOI 10.1109/TII.2017.2682101, IEEE Transactions on Industrial Informatics



the following equation:

$$f = \sum_{i=1}^{N} t_i + pC \tag{6}$$

where the fitness value $f$ consists of the PCO model objective function presented in (2) with the addition of a penalty factor. The constant $p$ represents the penalty value which is set to a high value. Finally, $C$ is a binary variable that is set to 1 if the LP sub-problem did not converge, otherwise it has a value equal to zero.

After evaluating each chromosome in the current population, two chromosomes with the best fitness values are selected by the GA operator to be used to produce the next generation while discarding the other chromosomes. The new generation is obtained by applying crossover and mutation to the selected chromosomes pair. This whole process is repeated until the required number of generations is achieved. The number of generations selected to solve each PCO model depends on the population size and the complexity of the system. It is worth noting that the penalty value can also affect the number of generations the algorithm requires to reach the optimal solution. Full description of the hybrid GA-LP technique is provided in [21].

## IV. Analysis of Different Coordination models

This section presents the results (optimal relay settings and optimal relay operating time) of all the models (refer to Table II) that are simulated and tested on both the 9-bus and the IEEE 14-bus systems. This is followed by a detailed analysis to investigate whether each simulated model is sufficient to guarantee proper DOCR coordination for near-end and far-end fault locations under all transients (single line/source outage contingencies) and mode of operations. Finally, by using the optimal relay settings that result in proper DOCR coordination, a breakdown of the relay operating times due to near-end and far-end faults on all the lines for both test systems is presented.

### A. Optimal DOCR Settings and Overall Time

In this subsection, the optimal relay settings obtained by simulating the models stated in Table II are analyzed. Each model takes into account a specific set of constraints that correspond to the amount of network topologies considered while solving the PCO model. Table III and Table IV present the optimal TDS and Ip settings for all the relays obtained by simulating each model for both the 9-bus and the IEEE 14-bus test systems, respectively. Furthermore, the objective value (penalty=0 since the LP problem converged for the presented solutions) corresponding to the simulated models for both test systems are presented in Table V.

It can be seen that in both test systems, the optimal relay settings obtained from solving each model are different. Moreover, the optimal TDS settings obtained for DOCRs installed in the IEEE 14-bus system are much higher than those attained for DOCRs in the 9-bus system (for presented models). This is due to the fact that the IEEE 14-bus system is highly looped and thus the problem is more complicated than the radial 9-bus system.

TABLE III
Optimal TDS and $I_p$ of Each model for the 9-Bus System

| Relay | model 1 | | model 2 | | model 3 | | model 4 | |
|---|---|---|---|---|---|---|---|---|
| | $TDS$ | $I_p$ | $TDS$ | $I_p$ | $TDS$ | $I_p$ | $TDS$ | $I_p$ |
| R1 | 0.309 | 0.5 | 0.166 | 2.0 | 0.316 | 0.5 | 0.322 | 0.5 |
| R2 | 0.068 | 2.0 | 0.156 | 1.0 | 0.065 | 2.5 | 0.343 | 0.6 |
| R3 | 0.205 | 0.6 | 0.137 | 1.5 | 0.166 | 1.0 | 0.195 | 0.8 |
| R4 | 0.054 | 2.5 | 0.133 | 1.5 | 0.076 | 2.5 | 0.437 | 0.5 |
| R5 | 0.100 | 1.0 | 0.110 | 0.8 | 0.081 | 1.5 | 0.121 | 0.8 |
| R6 | 0.066 | 2.5 | 0.160 | 1.5 | 0.088 | 2.5 | 0.496 | 0.5 |
| R7 | 0.050 | 0.5 | 0.050 | 0.5 | 0.050 | 0.5 | 0.050 | 0.8 |
| R8 | 0.050 | 1.5 | 0.050 | 1.5 | 0.058 | 1.5 | 0.101 | 1.5 |
| R9 | 0.139 | 2.5 | 0.168 | 2.0 | 0.308 | 0.5 | 0.321 | 0.5 |
| R10 | 0.050 | 2.5 | 0.110 | 1.5 | 0.074 | 2.5 | 0.380 | 0.5 |
| R11 | 0.108 | 2.5 | 0.181 | 1.0 | 0.150 | 1.5 | 0.195 | 0.8 |
| R12 | 0.092 | 1.0 | 0.124 | 0.8 | 0.176 | 0.8 | 0.071 | 1.5 |
| R13 | 0.064 | 2.5 | 0.133 | 0.6 | 0.120 | 0.8 | 0.117 | 0.8 |
| R14 | 0.111 | 1.0 | 0.111 | 1.0 | 0.056 | 1.5 | 0.078 | 1.5 |
| R15 | 0.050 | 0.5 | 0.050 | 0.6 | 0.050 | 0.6 | 0.050 | 0.5 |
| R16 | 0.050 | 1.5 | 0.050 | 1.5 | 0.063 | 1.5 | 0.085 | 1.5 |

TABLE IV
Optimal TDS and $I_p$ of Each model for the 14-Bus System

| Relay | model 1 | | model 2 | | model 3 | | model 4 | |
|---|---|---|---|---|---|---|---|---|
| | $TDS$ | $I_p$ | $TDS$ | $I_p$ | $TDS$ | $I_p$ | $TDS$ | $I_p$ |
| R1 | 0.224 | 2.5 | 0.286 | 2.5 | 0.409 | 2.0 | 1.757 | 0.8 |
| R2 | 0.159 | 2.5 | 0.238 | 2.5 | 0.235 | 2.5 | 1.685 | 0.6 |
| R3 | 0.231 | 1.5 | 0.411 | 1.0 | 0.442 | 1.0 | 1.370 | 1.0 |
| R4 | 0.207 | 2.5 | 0.333 | 2.5 | 0.415 | 2.5 | 2.122 | 0.6 |
| R5 | 0.202 | 2.5 | 0.495 | 0.6 | 0.484 | 0.8 | 1.816 | 0.5 |
| R6 | 0.171 | 2.5 | 0.377 | 1.0 | 0.420 | 1.5 | 1.861 | 0.5 |
| R7 | 0.253 | 2.5 | 0.362 | 2.0 | 0.623 | 0.6 | 2.147 | 0.5 |
| R8 | 0.157 | 2.5 | 0.217 | 2.5 | 0.329 | 2.5 | 1.680 | 0.8 |
| R9 | 0.158 | 2.5 | 0.233 | 2.5 | 0.424 | 1.0 | 1.311 | 1.0 |
| R10 | 0.128 | 2.5 | 0.185 | 2.5 | 0.228 | 2.5 | 0.968 | 2.0 |
| R11 | 0.231 | 2.5 | 0.348 | 2.0 | 0.341 | 2.0 | 2.053 | 0.8 |
| R12 | 0.271 | 2.5 | 0.359 | 2.5 | 0.501 | 2.5 | 1.704 | 1.5 |
| R13 | 0.314 | 2.5 | 0.547 | 2.0 | 0.715 | 1.0 | 1.864 | 2.0 |
| R14 | 0.329 | 2.5 | 0.544 | 1.5 | 0.560 | 2.5 | 2.062 | 2.0 |
| R15 | 0.209 | 2.5 | 0.277 | 2.5 | 0.342 | 2.5 | 1.061 | 2.5 |
| R16 | 0.129 | 2.5 | 0.215 | 2.5 | 0.388 | 1.0 | 1.483 | 0.8 |

TABLE V
Optimal Fitness Value of Each model For Both Test Systems

| System | Objective Values (seconds) | | | |
|---|---|---|---|---|
| | model 1 | model 2 | model 3 | model 4 |
| 9-bus | 11.239 | 11.579 | 14.105 | 17.841 |
| IEEE 14-bus | 8.3664 | 12.244 | 14.756 | 49.783 |

The changes in the optimal relay settings directly affects the optimal objective value (sum of all primary DOCRs due to near-end faults in the main topology) achieved in each model. As indicated in Table V, in both test systems, the optimal objective values achieved in models 2, 3, and 4 are higher than the value attained in model 1. This is due to the fact that in model 1, the PCO model is solved by considering only the main network topology, and thus the problem has a much lower number of constraints (the problem is relaxed) than the other models.

It can also be seen that for both test systems, the opti-

This article has been accepted for publication in a future issue of this journal, but has not been fully edited. Content may change prior to final publication. Citation information: DOI 10.1109/TII.2017.2682101, IEEE Transactions on Industrial Informatics



mal objective value obtained by considering the topologies corresponding to the two micro-grid operation modes (model 3) is higher than the optimal objective value attained by considering all the topologies resulting from single line outage contingencies (model 2). This can be explained in terms of the short circuit current. In model 3, it appears that the short circuit currents in the presence of grid connection are much higher than the case when grid connection is absent (islanded mode). Since the short circuit current passing through each relay is inversely proportional to the relay operating time, more strict coordination constraints are imposed in the PCO model to be able to simultaneously satisfy this wide range of coordination times. On the other hand, in model 2 the optimal objective value experiences a slight increase with respect to the optimal objective value obtained in model 1. This means that the short circuit currents do not vary significantly with the single line outage. Thus, although the number of constraints in model 2 is higher than those considered in model 3, the PCO model in model 2 tends to be more relaxed than in model 3 (due to reasons stated above) leading to a lower optimal objective value.

Another observation that can be made from Table V is that for the 9-bus and the IEEE 14-bus test systems, the optimal objective value achieved by considering all transients and operation conditions (model 4) is much higher (increase of 37% and 83.2% respectively) than the optimal objective value obtained by considering only the main topology (model 1).

### B. Coordination Constraints Violation Analysis

The optimal relay settings obtained by solving the PCO model of each model are tested for coordination of relay pairs across all topologies (from transients and operating conditions) that are derived from the main topology. The aim of this study is to determine the number of coordination violations occurring as a result of solving the PCO model while considering a particular set of constraints. The coordination of a relay pair is considered to be violated when the following situations occur:

1) The backup relay is set to operate after the primary relay operation time but with a time gap less than the CTI value (200 ms in this case).
2) The backup relay is set to operate before the primary relay operation time for a given fault.
3) The backup relay does not operate at all for its assigned fault.

For instance, Fig. 4 shows a zoomed in curves of the tripping characteristics of $R13$ and $R3$ due to the optimal settings attained from each model (Table IV). A bolted three-phase fault at $F14$ in the IEEE 14-bus system with outage of the DG at bus 5 results in a fault current of 3.19 kA passing through the primary $R13$ and its backup $R3$. Fig. 4a shows that by using model 1 optimal settings, $R13$ and $R3$ operation times are 0.6131 and 0.7251 s, respectively. Hence, coordination violation occurs because the backup $R3$ operates after the primary $R13$ but with a time gap of 112 ms, which is less than the 200 ms of the CTI. Similarly, Fig. 4b shows that by using model 2 optimal settings, $R13$ and $R3$ operation times are 1 and 1.08 s, respectively. Fig. 4c shows that by using model 3 optimal settings, $R13$ and $R3$ operation times are 1.09 and 1.17 s, respectively. Thus, in both model 2 and 3 cases, coordination violation occur because the backup $R3$ operates after the primary $R13$ but with a time gap of 80 ms, which is less than the 200 ms of the CTI. However, Fig. 4d shows that by using the proposed model 4 optimal settings, $R13$ and $R3$ operation times are 3.41 and 3.61 s, respectively. Accordingly, $R3$ and $R13$ are coordinated because the time gap between their respective operation is 200 ms.

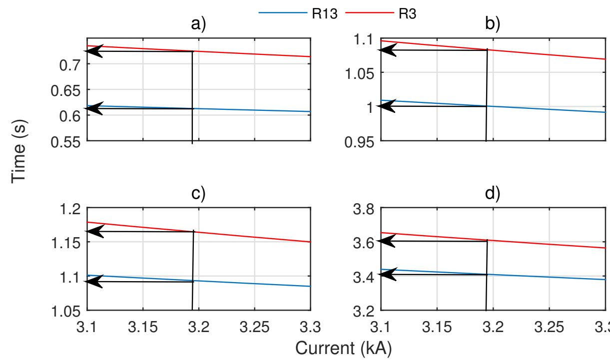


Fig. 4. The tripping characteristic curves of $R13$ and $R3$ due to the optimal settings attained from model a) 1, b) 2, c) 3, and d) 4.

TABLE VI
NUMBERS OF COORDINATION VIOLATIONS FOR THE 9-BUS SYSTEM

| Topology | Number of coordination violations | | | |
|---|---|---|---|---|
| | model 1 | model 2 | model 3 | model 4 |
| Main | 0 | 0 | 0 | 0 |
| Line 1-2 outage | 0 | 0 | 0 | 0 |
| Line 2-3 outage | 0 | 0 | 0 | 0 |
| Line 3-4 outage | 0 | 0 | 0 | 0 |
| Line 4-5 outage | 4 | 0 | 6 | 0 |
| Line 1-6 outage | 4 | 0 | 0 | 0 |
| Line 6-7 outage | 2 | 0 | 2 | 0 |
| Line 7-8 outage | 2 | 0 | 2 | 0 |
| Line 8-9 outage | 2 | 0 | 2 | 0 |
| Bus 4 DG outage | 5 | 3 | 7 | 0 |
| Bus 5 DG outage | 4 | 0 | 6 | 0 |
| Bus 6 DG outage | 4 | 4 | 4 | 0 |
| Bus 9 DG outage | 2 | 0 | 2 | 0 |
| Islanded mode | 4 | 4 | 0 | 0 |
| Total violations | 31 | 11 | 31 | 0 |

Table VI and Table VII present the detailed number of constraint violations as a result of considering the optimal settings corresponding to each model for the 9-bus and the IEEE 14-bus systems respectively. The total number of constraints that should be satisfied in the 9-bus and the IEEE 14-bus systems are 322 and 573 constraints, respectively.

It is clear that in both test systems, solving the PCO model based on model 4 (considering constraints resulting from all mentioned topologies) results in proper coordination for all DOCR pairs in each topology. However, models 1, 2, and 3 implemented in the 9-bus system experience coordination violations reaching 9.63%, 3.42%, and 9.63% respectively. Similarly, models 1, 2, and 3 implemented in the IEEE 14-bus system experience coordination violations reaching 20.6%, 6.12%, and 11.2% respectively. It can be seen that solving

This article has been accepted for publication in a future issue of this journal, but has not been fully edited. Content may change prior to final publication. Citation information: DOI 10.1109/TII.2017.2682101, IEEE Transactions on Industrial Informatics



TABLE VII
NUMBERS OF COORDINATION VIOLATIONS FOR THE 14-BUS SYSTEM

| Topology | Number of coordination violations | | | |
|---|---|---|---|---|
| | model 1 | model 2 | model 3 | model 4 |
| Main | 0 | 0 | 0 | 0 |
| Line 1-4 outage | 13 | 0 | 6 | 0 |
| Line 1-6 outage | 10 | 0 | 8 | 0 |
| Line 1-5 outage | 7 | 0 | 5 | 0 |
| Line 5-6 outage | 3 | 0 | 2 | 0 |
| Line 6-7 outage | 7 | 0 | 5 | 0 |
| Line 3-4 outage | 9 | 0 | 2 | 0 |
| Line 2-7 outage | 6 | 0 | 5 | 0 |
| Line 2-3outage | 9 | 0 | 3 | 0 |
| Bus 4 DG outage | 4 | 3 | 5 | 0 |
| Bus 5 DG outage | 6 | 5 | 7 | 0 |
| Bus 6 DG outage | 10 | 2 | 7 | 0 |
| Substation 1 outage | 12 | 8 | 5 | 0 |
| Substation 2 outage | 8 | 5 | 4 | 0 |
| Islanded mode | 14 | 12 | 0 | 0 |
| Total violations | 118 | 35 | 64 | 0 |

PCO model based on models 1, 2, or 3 for the IEEE 14-bus system will result in more coordination violations than for the 9-bus system.

It is also observed that in both test systems, DG and substation outage topologies have some coordination violations whenever models 1, 2, or 3 are considered. It appears that neither inclusion of topologies reflecting single line outage contingencies nor topologies obtained from islanded and grid-connected operation modes can satisfy DOCRs coordination in situations when DG or substation outage occur. These violations can be eliminated by considering all the topologies in models 2 and 3 in addition to the topologies resulting from single DG/substation outage contingencies (model 4) but at the expense of higher DOCR operation time as was discussed in section IV-A.

### C. Breakdown of Relay Operation Times

In this subsection, a breakdown of the DOCR operation times due to near-end and far-end faults on all the lines on the 9-bus and the IEEE 14-bus systems are presented in Tables VIII and IX, respectively. These tables show the DOCRs operation times obtained from the main topology for each system. Similar tables can be obtained for all other topologies, but they are not included in this paper for brevity.

In order to obtain the operation time of each DOCR, a short circuit analysis is performed on each system. Thus, the short circuit currents passing through each DOCR due to near-end and far-end faults are computed. Also, the optimal $TDS$ and $I_p$ settings of each DOCR is attained by solving the PCO model considering model 4 constraints since it is the only case that guarantees proper coordination for all considered topologies (as discussed in section IV-B). Finally, the optimal operating time of each relay is calculated by substituting the short circuit current, $TDS$, and $I_p$ settings of each DOCR into the inverse time current characteristic (equation 1). The results reveal that all primary/backup DOCR pairs are correctly coordinated within the CTI value (200 ms). Thus, directional

TABLE VIII
OPTIMAL PRIMARY AND BACKUP RELAY OPERATING TIMES FOR NEAR-END AND FAR-END FAULTS IN THE MAIN TOPOLOGY OF THE 9-BUS SYSTEM

| Fault location | Relays operating times (s) | | | |
|---|---|---|---|---|
| | Primary | | Backup | |
| F10 | R1 | 0.6859 | R10 | 1.2973 |
| | R2 | 1.3226 | R4 | 1.5263 |
| F11 | R1 | 0.7084 | R10 | 1.3652 |
| | R2 | 1.2997 | R4 | 1.5023 |
| F12 | R3 | 0.5084 | R1 | 0.7084 |
| | R4 | 1.5023 | R6 | 1.7054 |
| F13 | R3 | 0.5282 | R1 | 0.7317 |
| | R4 | 1.4789 | R6 | 1.6789 |
| F14 | R5 | 0.3282 | R3 | 0.5282 |
| | R6 | 1.6789 | R8 | 3.0958 |
| F15 | R5 | 0.3408 | R3 | 0.5485 |
| | R6 | 1.6532 | R8 | 2.7247 |
| F16 | R7 | 0.1302 | R5 | 0.3408 |
| | R8 | 2.7248 | — | — |
| F17 | R7 | 0.1356 | R5 | 0.3560 |
| | R8 | 2.5708 | — | — |
| F18 | R9 | 0.6885 | R2 | 1.3226 |
| | R10 | 1.2973 | R12 | 2.5251 |
| F19 | R9 | 0.7111 | R2 | 1.4008 |
| | R10 | 1.2772 | R12 | 2.1814 |
| F20 | R11 | 0.4794 | R9 | 0.7111 |
| | R12 | 2.1816 | R14 | 2.3954 |
| F21 | R11 | 0.4998 | R9 | 0.7383 |
| | R12 | 2.0423 | R14 | 2.2425 |
| F22 | R13 | 0.2998 | R11 | 0.4998 |
| | R14 | 2.2427 | R16 | 2.4555 |
| F23 | R13 | 0.3124 | R11 | 0.5208 |
| | R14 | 2.1082 | R16 | 2.3082 |
| F24 | R15 | 0.1124 | R13 | 0.3124 |
| | R16 | 2.3083 | — | — |
| F25 | R15 | 0.1163 | R13 | 0.3252 |
| | R16 | 2.1778 | — | — |

TABLE IX
OPTIMAL PRIMARY AND BACKUP RELAY OPERATING TIMES FOR NEAR-END AND FAR-END FAULTS IN THE MAIN TOPOLOGY OF THE 14-BUS SYSTEM

| Fault location | Relays operating times (s) | | | | | |
|---|---|---|---|---|---|---|
| | Primary | | Backup 1 | | Backup 2 | |
| F8 | R1 | 3.0510 | R4 | 4.3472 | R6 | 3.9807 |
| | R2 | 3.8398 | R11 | 5.4094 | — | — |
| F9 | R1 | 3.9028 | R4 | 5.8124 | R6 | 6.1540 |
| | R2 | 3.1769 | R11 | 4.1101 | — | — |
| F10 | R5 | 2.8009 | R2 | 3.8398 | R4 | 4.3472 |
| | R6 | 3.9807 | R13 | 17.7317 | R16 | 5.6962 |
| F11 | R5 | 3.4068 | R2 | 4.9096 | R4 | 7.4305 |
| | R6 | 3.2255 | R13 | 3.9445 | R16 | 4.2440 |
| F12 | R3 | 2.4448 | R2 | 3.8398 | R6 | 3.9807 |
| | R4 | 4.3472 | R14 | 19.6153 | — | — |
| F13 | R3 | 3.6111 | R2 | 5.1817 | R6 | 7.0061 |
| | R4 | 3.2135 | R14 | 3.9271 | — | — |
| F14 | R13 | 2.9498 | R3 | 3.6111 | — | — |
| | R14 | 3.9271 | R5 | 6.8366 | R16 | 6.0038 |
| F15 | R13 | 3.9445 | R3 | 16.6200 | — | — |
| | R14 | 2.9674 | R5 | 3.4068 | R16 | 4.2440 |
| F16 | R15 | 2.4378 | R5 | 3.4068 | R13 | 3.9445 |
| | R16 | 4.2440 | R9 | 4.7978 | — | — |
| F17 | R15 | 3.9741 | R5 | 5.3003 | R13 | 6.0246 |
| | R16 | 3.2493 | R9 | 3.4581 | — | — |
| F18 | R11 | 3.5461 | R7 | 3.7493 | — | — |
| | R12 | 3.9149 | R1 | 5.0563 | — | — |
| F19 | R11 | 4.1101 | R7 | 4.3526 | — | — |
| | R12 | 3.2199 | R1 | 3.9028 | — | — |
| F20 | R9 | 2.5680 | R8 | 3.9844 | — | — |
| | R10 | 5.4074 | R15 | 5.6291 | — | — |
| F21 | R9 | 3.4581 | R8 | 6.5149 | — | — |
| | R10 | 3.7606 | R15 | 3.9741 | — | — |
| F22 | R7 | 3.4645 | R10 | 5.4074 | — | — |
| | R8 | 3.9844 | R12 | 4.2195 | — | — |
| F23 | R7 | 3.7493 | R10 | 8.0755 | — | — |
| | R8 | 3.7075 | R12 | 3.9149 | — | — |

overcurrent relays are capable of protecting microgrids under various conditions and network topologies.

Moreover, the DOCR operating times in the 14-bus system are much higher than the ones in the 9-bus system because the

This article has been accepted for publication in a future issue of this journal, but has not been fully edited. Content may change prior to final publication. Citation information: DOI 10.1109/TII.2017.2682101, IEEE Transactions on Industrial Informatics



latter system is larger and more complex. For large systems where the DOCRs operating times are expected to increase, further reduction of the DOCR operating times can be possibly achieved by replacing the conventional relay inverse-time-current characteristic in (1) with new characteristics such as the time-current-voltage characteristic [9], the dual-setting current characteristic [9], or any other non-standard tripping characteristic [35]. Another possibility would be to rely on a low bandwidth communication link where the system topology is detected and accordingly the optimal DOCR settings are adaptively changed.

## V. Conclusion

While designing a microgrid protection scheme, it is essential to consider all the possible network topologies as a result of transients and operation conditions. In this paper, the optimal DOCRs settings for a microgrid are determined considering all network topologies obtained from single line, DG, and substation outage contingencies (transients) in addition to the grid-connected and islanded topologies simultaneously. Basically, the protection coordination problem is formulated as a MINLP problem with a set of coordination constraints that includes all of the mentioned topologies. The proposed method was solved and compared against three other models. These models involve solving the protection coordination problem by considering the main topology only, single line outage contingencies, or microgrids dual-topologies. The results show that directional overcurrent relays can be optimally set, for microgrids, to accommodate multiple network topologies under the various aforementioned contingencies.

## References


[1] J. L. Blackburn and T. J. Domin, *Protective relaying: principles and applications*. CRC press, 2015.

[2] J. H. Teng, "Unsymmetrical short-circuit fault analysis for weakly meshed distribution systems," *IEEE Trans. Power Syst.*, vol. 25, no. 1, pp. 96–105, Feb 2010.

[3] Q. Yang, J. A. Barria, and T. C. Green, "Communication infrastructures for distributed control of power distribution networks," *IEEE Trans. Ind. Informat.*, vol. 7, no. 2, pp. 316–327, May 2011.

[4] B. Hussain, S. M. Sharkh, and S. Hussain, "Impact studies of distributed generation on power quality and protection setup of an existing distribution network," in *SPEEDAM 2010*, June 2010, pp. 1243–1246.

[5] H. H. Zeineldin, Y. A. R. I. Mohamed, V. Khadkikar, and V. R. Pandi, "A protection coordination index for evaluating distributed generation impacts on protection for meshed distribution systems," *IEEE Trans. Smart Grid*, vol. 4, no. 3, pp. 1523–1532, Sept 2013.

[6] V. R. Pandi, H. H. Zeineldin, and W. Xiao, "Determining optimal location and size of distributed generation resources considering harmonic and protection coordination limits," *IEEE Trans. Power Syst.*, vol. 28, no. 2, pp. 1245–1254, May 2013.

[7] W. El-Khattam and T. S. Sidhu, "Restoration of directional overcurrent relay coordination in distributed generation systems utilizing fault current limiter," *IEEE Trans. Power Del.*, vol. 23, no. 2, pp. 576–585, April 2008.

[8] W. K. A. Najy, H. H. Zeineldin, and W. L. Woon, "Optimal protection coordination for microgrids with grid-connected and islanded capability," *IEEE Trans. Ind. Electron.*, vol. 60, no. 4, pp. 1668–1677, April 2013.

[9] K. A. Saleh, H. H. Zeineldin, A. Al-Hinai, and E. F. El-Saadany, "Optimal coordination of directional overcurrent relays using a new time–current–voltage characteristic," *IEEE Trans. Power Del.*, vol. 30, no. 2, pp. 537–544, April 2015.

[10] K. Saleh, H. Zeineldin, A. Al-Hinai, and E. F. El-Saadany, "Dual-setting characteristic for directional overcurrent relays considering multiple fault locations," *IET Generation, Transmission Distribution*, vol. 9, no. 12, pp. 1332–1340, 2015.

[11] K. A. Saleh, M. S. E. Moursi, and H. H. Zeineldin, "A new protection scheme considering fault ride through requirements for transmission level interconnected wind parks," *IEEE Trans. Ind. Informat.*, vol. 11, no. 6, pp. 1324–1333, Dec 2015.

[12] L. Huchel and H. H. Zeineldin, "Planning the coordination of directional overcurrent relays for distribution systems considering dg," *IEEE Trans. Smart Grid*, vol. 7, no. 3, pp. 1642–1649, May 2016.

[13] B. Chattopadhyay, M. S. Sachdev, and T. S. Sidhu, "An on-line relay coordination algorithm for adaptive protection using linear programming technique," *IEEE Trans. Power Del.*, vol. 11, no. 1, pp. 165–173, Jan 1996.

[14] A. J. Urdaneta, H. Restrepo, S. Marquez, and J. Sanchez, "Coordination of directional overcurrent relay timing using linear programming," *IEEE Trans. Power Del.*, vol. 11, no. 1, pp. 122–129, Jan 1996.

[15] A. J. Urdaneta, L. G. Perez, and H. Restrepo, "Optimal coordination of directional overcurrent relays considering dynamic changes in the network topology," *IEEE Trans. Power Del.*, vol. 12, no. 4, pp. 1458–1464, Oct 1997.

[16] A. Urdaneta, L. Perez, J. Gomez, B. Feijoo, and M. Gonzalez, "Presolve analysis and interior point solutions of the linear programming coordination problem of directional overcurrent relays," *International Journal of Electrical Power & Energy Systems*, vol. 23, no. 8, pp. 819–825, 2001.

[17] A. S. Noghabi, H. R. Mashhadi, and J. Sadeh, "Optimal coordination of directional overcurrent relays considering different network topologies using interval linear programming," *IEEE Trans. Power Del.*, vol. 25, no. 3, pp. 1348–1354, July 2010.

[18] D. Birla, R. P. Maheshwari, and H. O. Gupta, "A new nonlinear directional overcurrent relay coordination technique, and banes and boons of near-end faults based approach," *IEEE Trans. Power Del.*, vol. 21, no. 3, pp. 1176–1182, July 2006.

[19] P. P. Bedekar and S. R. Bhide, "Optimum coordination of directional overcurrent relays using the hybrid ga-nlp approach," *IEEE Trans. Power Del.*, vol. 26, no. 1, pp. 109–119, Jan 2011.

[20] H. Zeineldin, E. El-Saadany, and M. Salama, "Optimal coordination of overcurrent relays using a modified particle swarm optimization," *Electric Power Systems Research*, vol. 76, no. 11, pp. 988–995, 2006.

[21] A. S. Noghabi, J. Sadeh, and H. R. Mashhadi, "Considering different network topologies in optimal overcurrent relay coordination using a hybrid ga," *IEEE Trans. Power Del.*, vol. 24, no. 4, pp. 1857–1863, Oct 2009.

[22] U. F. E. R. Commission *et al.*, "Mandatory reliability standards for the bulk-power system," *Order*, no. 693, p. 72, Apr. 2007.

[23] H. Zhang, G. T. Heydt, V. Vittal, and J. Quintero, "An improved network model for transmission expansion planning considering reactive power and network losses," *IEEE Trans. Power Syst.*, vol. 28, no. 3, pp. 3471–3479, Aug 2013.

[24] B. Cova, N. Losignore, P. Marannino, and M. Montagna, "Contingency constrained optimal reactive power flow procedures for voltage control in planning and operation," *IEEE Trans. Power Syst.*, vol. 10, no. 2, pp. 602–608, May 1995.

[25] M. Khanabadi, H. Ghasemi, and M. Doostizadeh, "Optimal transmission switching considering voltage security and n-1 contingency analysis," *IEEE Trans. Power Syst.*, vol. 28, no. 1, pp. 542–550, Feb 2013.

[26] A. J. Urdaneta, R. Nadira, and L. G. P. Jimenez, "Optimal coordination of directional overcurrent relays in interconnected power systems," *IEEE Trans. Power Del.*, vol. 3, no. 3, pp. 903–911, Jul 1988.

[27] N. Nimpitiwan, G. T. Heydt, R. Ayyanar, and S. Suryanarayanan, "Fault current contribution from synchronous machine and inverter based distributed generators," *IEEE Trans. Power Del.*, vol. 22, no. 1, pp. 634–641, Jan 2007.

[28] IEC, "Relays, single input energizing quality measuring with dependent or independent," 1989.

[29] T. Areva, "Network protection & automation guide," *Flash Espace, Cayfosa*, pp. 123–151, 2002.

[30] J. B. Manuel, H. E. L. Zavala, E. A. Ramrez, D. S. Escobedo, and H. J. Altuve, "Protecting distribution feeders for simultaneous faults," in *2010 63rd Annual Conference for Protective Relay Engineers*, March 2010, pp. 1–9.

[31] "Ieee recommended practice for protection and coordination of industrial and commercial power systems (ieee buff book)," *IEEE Std 242-2001 (Revision of IEEE Std 242-1986) [IEEE Buff Book]*, pp. 1–710, Dec 2001.

[32] D. Durand and D. Pieniazek, "Overcurrent protection & coordination for industrial applications," *2010 Industry applications society annual meeting*, Oct. 2010.

[33] E. Dick and A. Narang, "Canadian urban benchmark distribution systems," *Report# CETC-Varennes*, vol. 121, 2005.

[34] University of Washington, Seattle, "Power Systems Test Case Archive," 2016. [Online]. Available: http://www2.ee.washington.edu/research/pstca/

[35] Y. Damchi, J. Sadeh, and H. R. Mashhadi, "Optimal coordination of distance and overcurrent relays considering a non-standard tripping characteristic for distance relays," *IET Generation, Transmission Distribution*, vol. 10, no. 6, pp. 1448–1457, 2016.

**Khaled A. Saleh** (S'12) was born in Cairo, Egypt, in 1991. He received the B.Sc. degree in electrical engineering from The Petroleum Institute, Abu Dhabi, UAE, in 2012; and the M.Sc. degree in electrical power engineering from Masdar Institute of Science and Technology, Abu Dhabi, UAE, in 2014. Currently, he is pursuing the Ph.D. degree at the Electrical and Computer Engineering Department, University of Waterloo, Waterloo, ON, Canada.

His research interests include AC and DC power systems protection, travelling-wave based protection, distributed and renewable generation protection, DC grids, and optimization and digital signal processing techniques application to power systems.

**H. H. Zeineldin** (M06 SM13) received the B.Sc. and M.Sc. degrees in electrical engineering from Cairo University, Cairo, Egypt, in 1999 and 2002, respectively, and the Ph.D. degree in electrical and computer engineering from the University of Waterloo, Waterloo, ON, Canada, in 2006.

He was with Smith and Andersen Electrical Engineering, Inc., North York, ON, where he was involved in projects involving distribution system design, protection, and distributed generation. He was a Visiting Professor with the Massachusetts Institute of Technology, Cambridge, MA, USA. He is with the Faculty of Engineering, Cairo University and is currently a Professor with the Masdar Institute of Science and Technology, Abu Dhabi, UAE. His current interests include distribution system protection, distributed generation, and micro-grids. Dr. Zeineldin is currently an Editor of the IEEE TRANSACTIONS ON ENERGY CONVERSION and the IEEE TRANSACTIONS ON SMART GRID.

**Ehab F. El-Saadany** (SM05) was born in Cairo, Egypt, in 1964. He received the B.Sc. and M.Sc. degrees in electrical engineering from Ain Shams University, Cairo, Egypt, in 1986 and 1990, respectively, and the Ph.D. degree in electrical engineering from the University of Waterloo, Waterloo, ON, Canada, in 1998. Currently, he is a Professor with the Department of Electrical and Computer Engineering, University of Waterloo.

His current research interests include distribution system operation and control, distributed generation, smart-grid applications, self-healing mechanisms, power quality, and microelectromechanical-systems micropower generators. Dr. El-Saadany is the holder of the Canada Research Chair in Smart Distribution Systems in recognition of his contributions to the areas of distributed generation and microgrids. He is the Editor in the IEEE TRANSACTIONS ON SMART GRID.